Alma Mater Studiorum Università di Bologna
Archivio istituzionale della ricerca

Enantioselective CO2 Fixation Via a Heck-Coupling/Carboxylation Cascade Catalyzed by Nickel

Enantioselective CO₂ Fixation Via a Heck-Coupling/Carboxylation Cascade Catalyzed by Nickel

Alessandro Cerveri,[a] Riccardo Giovanelli,[a] Davide Sella,[a] Riccardo Pedrazzani,[a] Magda Monari,[a] Olalla Nieto Faza,[b] Carlos Silva López,*[b] Marco Bandini*[a,c]

[a] Mr. A. Cerveri, Mr. R. Giovanelli, Mr. D. Sella, Mr. R. Pedrazzani, Prof. M. Monari, Prof. M. Bandini Corresponding Author(s)
Dipartimento di Chimica "Giacomo Ciamician"
Alma Mater Studiorum – Università di Bologna
Via Selmi 2, 40126, Bologna, Italy
E-mail: marco.bandini@unibo.it

[b] Dr. O. Nieto Faza, Prof. C. Silva López
Departamento de Química Orgánica
Universidade de Vigo
As Lagoas (Marcosende), 36310, Spain
Email: carlos.silva@uvigo.es

[c] Prof. M. Bandini
Consorzio CINMPIS
via Selmi 2, 40126, Bologna, Italy

Supporting information for this article is given via a link at the end of the document.((Please delete this text if not appropriate))

Abstract: A novel asymmetric nickel-based procedure has been developed in which CO₂ fixation is achieved as a second step of a truncated Heck coupling. For this, a new chiral ligand has been prepared and shown to achieve enantiomeric excesses up to 99%. The overall process efficiently furnishes chiral 2,3-dihydrobenzofuran-3-ylacetic acids, an important class of bioactive products, from easy to prepare starting materials. A combined experimental and computational effort revealed the key steps of the catalytic cycle and suggested the unexpected participation of Ni(I) species in the coupling event.

The interest in carbon dioxide in organic synthetic methodology as a valuable and desirable C1-synthon, is experimenting an exponential growth.[1] Its low toxicity, abundance and reduced cost are unquestionable "pros" supporting its use, which usually counterbalance some major "cons" such as high-activation barriers and low solubility in organic solvents. Over the past decade, incredible steps towards the chemoselective catalytic electrophilic as well as nucleophilic activation of CO₂ have been taken, making the selective incorporation of CO₂ in organic scaffolds accessible in synthetically useful manners.[2]

In organic synthesis, catalytic carboxylation[3] and carbonylation[4] protocols, based on a low-pressure CO₂ atmosphere, represent important cornerstones in the creation of chemical complexity/diversity via C1-homologation reactions. However, despite the titanic efforts deployed in this direction by means of metal-based and metal-free catalysis, the realization of added-value compounds via enantioselective CO₂-based catalytic carboxylation reactions is still far from being fully developed.[5]

In this context, the enantiopure 2,3-dihydrobenzofuran-3-ylacetic acid scaffold **A** (Figure 1) is of pivotal importance in naturally occurring compounds.[6] However a direct and stereoselective catalytic approach to this motif has not been found yet.[7] In continuation with our research program focused on CO₂ fixation procedures[8a] and Ni-catalyzed cross-coupling reactions,[8b-d] we envisioned the possibility to apply metal catalyzed CO₂ fixation reactions[9] to the direct synthesis of motif **A**, and an unprecedented Ni-catalyzed intramolecular reductive

Heck-coupling[10,11] followed by CO₂-based carboxylation was mustered to this end.
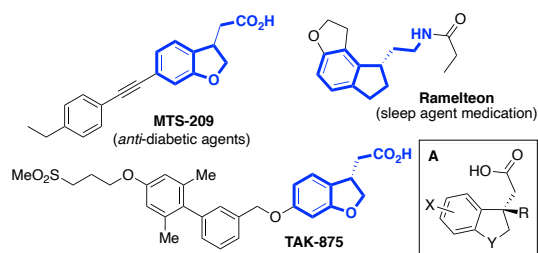
Figure 1. Examples of bio-active compounds featuring 2,3-dihydrobenzofuran-3-ylacetic acid scaffold **A** and analogues.

It is worth mentioning that, although a number of enantioselective metal catalyzed truncated Heck-couplings have been reported (Scheme 1a),[12] the use of CO₂ as the final "electrophilic" trapping agent of the *in situ* generated organometallic intermediate has never been associated so far to this methodology.
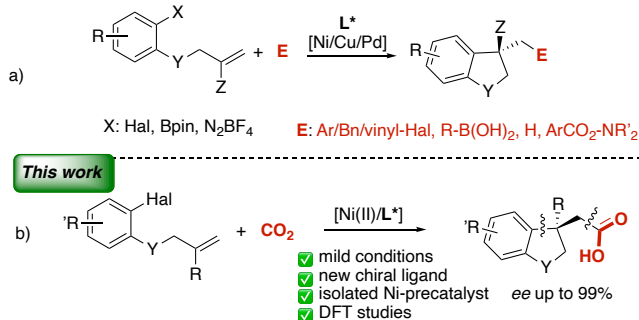
Scheme 1. State of the art and present working plan for the enantioselective synthesis of the 2,3-dihydrobenzofuran scaffold.

In this paper, we present our recent findings in the enantioselective (*ee* up to 99%) tandem Heck-coupling / carboxylation protocol with CO_2 by means of an air stable and fully characterized chiral Ni-pyridyl imidazolyl pre-catalyst. The reaction mechanism has been addressed through a combination of experimental and computational studies, enabling what is proposed to be a Ni(I)-assisted truncated Heck-coupling event, along with a stereodiscrimination model based of non-covalent interactions at the stereo-determining transition states.

At the outset of the investigation, we envisioned that iodo-arylether **1a** could act as a suitable model acyclic precursor to yield the desired dihydrobenzofuran-3-ylacetic acid scaffold under reductive cross-coupling/carboxylative conditions. Targeting abundant and low toxic 3d-TMs as catalysts, nickel complexes were assessed along with a survey of reaction parameters. Delightfully, the use of the *in situ* formed **L3**/NiI$_2$ (20/10 mol%) pre-catalyst, Zn (3 eq) as reducing agent, TMSCl (3 eq) and TBAI (20 mol%) as additives, released the desired benzofused acetic acid (*R*)-**2a** in 52% yield and 93% *ee* via exposure to an atmosphere of CO_2 in DMF (0.07 mM, rt, 16 h, Table 1 entry 3). The main by-products **i-iv** (Scheme of Table 1) were identified in variable amounts in the Ni-catalysis and accounts for the moderate yield.

Table 1. Optimization reaction conditions.[a]
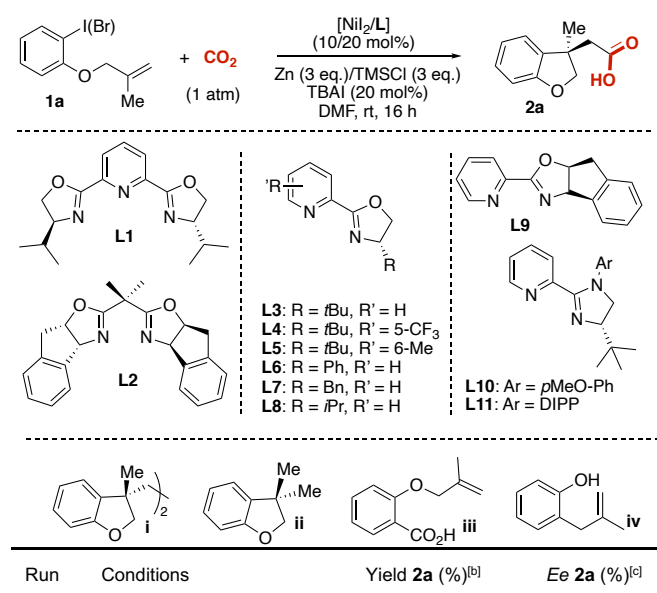
Run	Conditions	Yield **2a** (%)[b]	*Ee* **2a** (%)[c]
1	**L1**	traces	ND
2	**L2**	13	-21[d]
3	**L3**	52	93
4	**L4**	Traces	ND[e]
5	**L5**	8	-7
6	**L6**	18	41
7	**L7**	Traces	ND
8	**L8**	30	71
9	**L9**	11	-72[d]
10	**L10**	36	90
11	**L11**	58	96
12	**L11**/NiBr$_2$•DME	66	96
13	**L11**/ NiCl$_2$•glyme	60	93
14	No TMSCl	NR	--
15	No CO_2	NR	--
16	No TBAI	47	96
17[f]	0 °C	31	98
18[g]	60 °C	14	95
19	Mn instead of Zn	traces	ND
20	Br-**1a** was used	43	97

[a] Reaction conditions: **1a** (0.07 M). Under anhydrous conditions. [b] Determined after flash chromatography. [c] Determined via chiral HPLC. The absolute configuration of **2a** was determined via X-Ray analysis (*vide infra*). [d] Inverted stereoinduction was observed. nr: no reaction. nd: not determined. [e] By-products derived from dehalogenation, rearrangement and dimerization of de-iodinated **1a** were isolated as major outcomes. [f] By-product **III** (ref 12) was isolated in 56% yield. [g] Substantial decomposition of the starting material was recorded. DME: dimethoxyethane.

From the screening of reaction conditions, the use of C2-symmetric chiral PyBox **L1** and Box **L2** ligands did not yield synthetically useful results (entries 1,2). The introduction of an electron-withdrawing unit into the C1-symmetric PyOx (*i.e.* CF$_3$, **L4**) at the C5-position of the pyridyl ring resulted in a marked degrading of chemical outcomes (entry 4). The presence of a mild donor with reduced steric volume (*i.e.* Me, **L5**) in proximity to the coordinating pyridyl nitrogen atom proved not only highly detrimental for the turnover of the process but also led to an inversion of the stereochemical induction (see SI for computational analysis). Modifying the *t*Bu steric probe on the oxazoline framework also produced undesired effects (**L6-L9**). In order to test if more profound changes to the electronic structure of the ligand would improve the output of this process, we tested some imidazoline variants (**L10-L11**). Gladly, the replacement of PyOx **L3** with pyridyl imidazoline ligand **L11** (DIPP: 2,6-*i*Pr-phenyl)[13] resulted in substantial improvements in both reproducibility and chemical outcomes (yield = 66%, *ee* = 96%) in the presence of NiBr$_2$•DME (entry 12). Focusing on the role of additives, the use of catalytic amounts (20 mol%) of TBAI (tetrabutylammonium iodide) improved the turnover of the process (yield = 47%, *ee* = 96%, entry 16) likely facilitating the release of the metal from the final carboxylates. Even more pronounced was found to be the impact of TMSCl on the mechanism (entry 14): its omission caused complete inhibition of the process. This can be attributed to multiple actions such as: i) activation of the metal powder reductant; ii) co-activation of the CO_2 and iii) metal scavenging of the final carboxylates. Room temperature led to optimal results with respect to 0 °C or 60 °C (entries 17,18) and Zn as a stoichiometric sacrificial metal reductant proved superior to Mn (entry 19). Finally, the bromo derivative Br-**1a** could also be employed as a model substrate, although at the expense of a light decrease in the chemical yield (yield = 43%, *ee* = 97%, entry 20).

In an attempt to simplify the protocol and in order to get further insight into the real nature of the catalytically active chiral Ni complex, we envisioned the possibility of using a pre-formed

Ni-adduct in the carboxylation event. Here, the synthesis of **L11**-NiCl$_2$ was attempted by refluxing in THF a 2:1 mixture of **L11** and dried NiCl$_2$. Interestingly, a single-crystal X-ray study carried out on one crystal grown from the resulting pale-green solid revealed the formation of the cationic aquo complex [(**L11**)$_2$Ni(H$_2$O)Cl]$^+$(Cl$^-$ as counterion). The Ni(II) center exhibits a distorted octahedral geometry (Figure 2a, Figure S2) being coordinated by one chloride, one H$_2$O molecule and two pairs of N atoms of the bidentate **L11** ligand. The Cl$^-$ and H$_2$O ligands are in mutual *cis* position whereas in the bidentate NˆN ligands (**L11**) the pyridyl N atoms adopt a *trans* arrangement and the imidazolyl N atoms have a *cis* disposition.
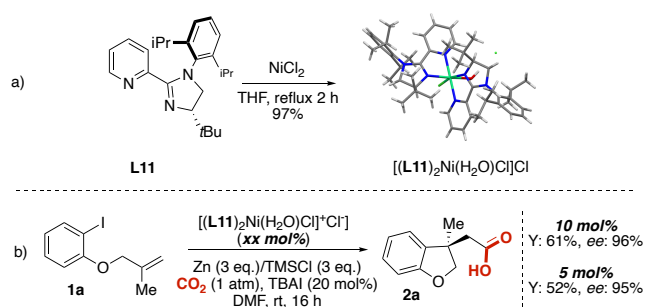
Figure 2. Synthesis of aquo [(**L11**)$_2$Ni(H$_2$O)Cl]Cl adduct and employment in the enantioselective carboxylative Heck-coupling.

The Ni-N$_{py}$ distances [2.073 and 2.084(3) Å] are similar and shorter than the Ni-N$_{im}$ ones [2.092 and 2.122(3) Å] being the latter N atom positioned *trans* to the chloride ligand. The Ni-O and Ni-Cl distances [2.126 and 2.141(3) Å] fall in the range typical for Ni complexes. The N$_{py}$-Ni-N$_{im}$ bite angles in the two five-membered metallacycles are almost identical [78.4(2) and 77.8(1)°, respectively]. The pyridyl and imidazoline rings in each **L11** ligand are not coplanar but have dihedral angles of 18.2 and 17.7(2)°, respectively, due to steric congestion generated by the bulky substituents.

Interestingly, this cationic aquo complex [(**L11**)$_2$Ni(H$_2$O)Cl]Cl (5-10 mol%) proved high competence in promoting the carboxylative truncated Heck-coupling of **1a** delivering the dihydrobenzofuran **2a** in similar extent to the *in situ* approach (Figure 2b *vs* entry 13, Table 1).

Having established the optimal reaction conditions, the generality of the enantioselective carboxylative Heck cross-coupling was assessed by subjecting a range of diversely functionalized *ortho*-aryliodines (**1b**-**s**) to the cascade protocol in the presence of [(**L11**)$_2$Ni(H$_2$O)Cl]Cl (10 mol%). The chemical outcomes of these essays have been collected in Scheme 2a-d and from the results some preliminary conclusions can be drawn.

Tolerance towards decoration of the phenolic ring with electron-donating substituents (Me, *i*Pr, *t*Bu) was recorded through substrates **1b**-**j**. In particular, the corresponding 2,3-dihydrobenzofuran-3-ylacetic acids **2b**-**j** were isolated in synthetically useful yields (61-69%) and enantiomeric excesses systematically higher than 90% were obtained (Scheme 2a/b). On

the contrary, limitations of the method emerged from the accommodation of EWGs at the aromatic ring (*i.e.* 4-Cl, 4-CF$_3$) that prevalently led to the direct carboxylation of the benzene ring, prevalently.[14]

The possibility to decorate the newly formed all carbon quaternary stereogenic centers with different substituents was then considered (Scheme 2c). In particular, aliphatic, aromatic and OMe groups were successfully installed at different distances from the stereocenter (**2k-o**) resulting in similar and remarkable chemical and optical outcomes (*ee* up to 98%). Finally, the role of the tethering unit was investigated by replacing the oxygen atom with *C*- as well as *N*-based connectors (**2p-s**, Scheme 2d). Here, although *N*-allyl- and *N*-Boc-indoline scaffolds **2p-r** were isolated in moderate extents (*ee*: 11-69%), the enantio-enriched dihydroindene acetic acid **2s** was obtained in excellent stereochemical yield (*ee* = 98%). Then, the absolute configuration of compound **2a** was unambiguously determined to be *R* via single crystal X-ray analysis of the corresponding bromo-amide **3a** (Scheme 2e). Additionally, the pivotal role of CO$_2$ in generating the carboxylic unit of targeted compounds **2** was determined via a labelled ^{13}C-experiment. As a matter of fact, a full incorporation of ^{13}C-carbon dioxide (99.8% labelling) was obtained in the final compound **2a** when ^{13}CO$_2$ was employed under optimal reaction conditions (^{13}C-**2a**, yield = 65%, *ee* = 98%, Scheme 2f).

In order to gain further insight into this reaction, a mechanistic exploration was carried out in parallel by DFT simulations (detailed methodology can be found in the Supporting Information).[15] Several questions that are key to the understanding of this reactivity are, at least: 1- what is the structural model of enantiodiscrimination, 2- which is the active catalyst and 3- how the fundamental role of the solvent can be explained.[16]

Initially we assumed that the [(**L**)$_2$Ni(H$_2$O)Cl]Cl complex, with a 2:1 **L**:Ni ratio, would dissociate delivering the **L**Ni species **I** as the active catalyst (*see* the NLE experiment).[17] We also assumed that [Ni(0)] would be the oxidation state of the catalyst, after reduction with the excess of zinc.[18] Catalytic cycles were simulated via DFT calculations (for computational details see the Supporting Information) for the PyOx (**L3**) and its imidazoline variant **L11**. Both ligands yielded similar reaction profiles. First we explored a [Ni(0)]/[Ni(II)] catalytic cycle in which Zn would only participate at the end, to restore the active [Ni(0)] catalyst **I** (path A - red zone in Scheme 3). From this, a facile oxidative addition of **1a** occurs to form intermediate **II**. Then, the stereodiscriminating addition of the Ni-C bond to the alkene must occur. The barriers associated to the formation of the two diastereomers favor (by 2.5 kcal/mol) the formation of intermediate **III**. We attempted to describe this step also on the neutral complex **II** but we could only find the associated transition state assuming prior loss of iodine. This is explained through the need to open a coordinating vacant site such that the double bond can be pre-activated for the addition step. However, the insertion of CO$_2$ onto intermediates **III** and **III-diast**, to yield the final carboxylates **IV** and **IV-diast**, featured high activation energies (26.3 and 36.7 kcal/mol, respectively) rendering these paths unlikely.

3
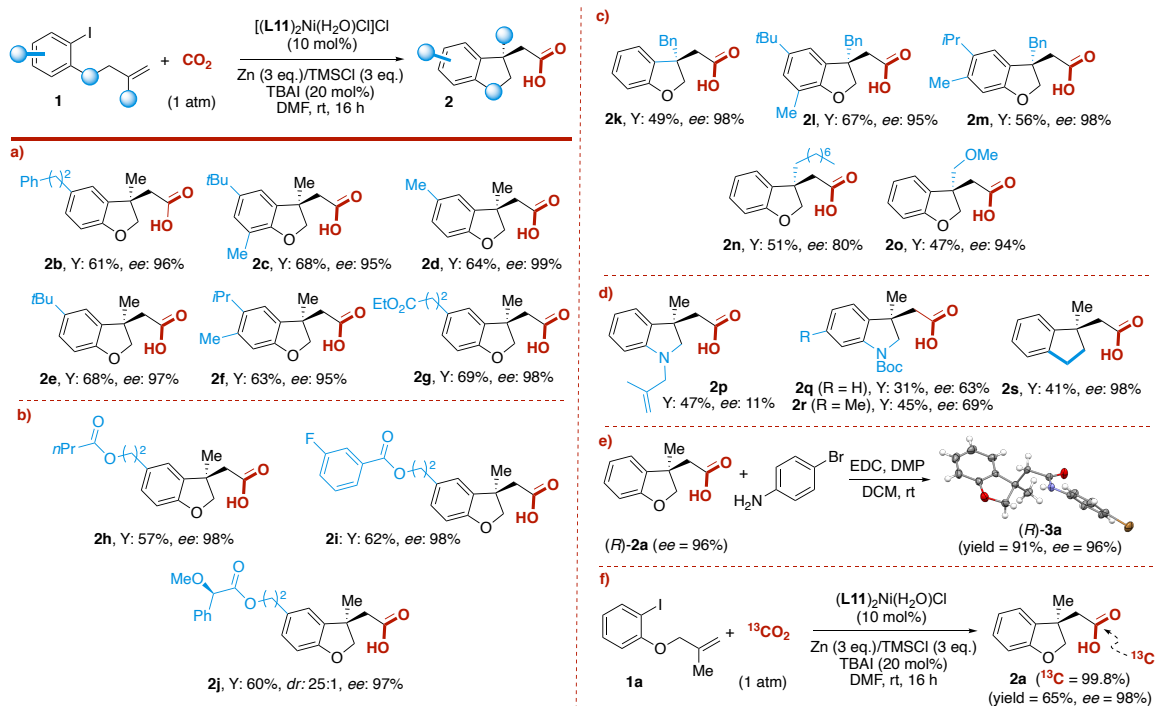
Scheme 2. Substrate scope of the present Heck-carboxylation cascade reaction (a-d). Absolute configuration determination (e) and labelling isotopic experiment (f).

We therefore decided to analyze whether a zinc-mediated [Ni(II)]/[Ni(I)] reduction step along the reaction pathway could facilitate the carboxylation event,[19] and indeed, the reaction proceeds much more favorably if Ni is reduced right before CO_2 insertion (path B - yellow block in Scheme 3). This reduction step could also be occurring earlier in the mechanism, right after the oxidative addition (path C - yellow block in Scheme 3). Interestingly the latter alternative, which involves a rare Heck step occurring at a Ni(I) species, also produces very competitive barriers for the subsequent steps.

To be able to determine which, of these two alternative pathways (B or C), is more plausible and at what point along the mechanism the reduction step is operating, we analyzed our experimental results in detail. While doing so we realized that one very common side product of this protocol is the benzoic acid derivative (**SP**)[14] deriving by a direct carboxylation of the aryl-Ni intermediates. We therefore computed the transition state for this carboxylation both at the [Ni(II)] and [Ni(I)] complexes. We found that this step is very costly for the [Ni(II)] complex (a computed barrier of about 30 kcal/mol) and that it is feasible when acting on the [Ni(I)] species.[18] These results therefore not only help explain the formation of this byproduct but also strongly candidate the path B - yellow block in Scheme 3 as the mechanism at work, involving an unusual Heck step on a [Ni(I)] complex.[20]

In an attempt to unequivocally determine the nature of the active catalyst, we performed a non-linear effect study[17]

on the model transformation **1a** → **2a**, by varying the enantiopurity of the chiral ligand **L3**. Interestingly, a perfect linear correlation between *ee*(**L3**) and *ee*(**2a**) was observed (see Figure S1).
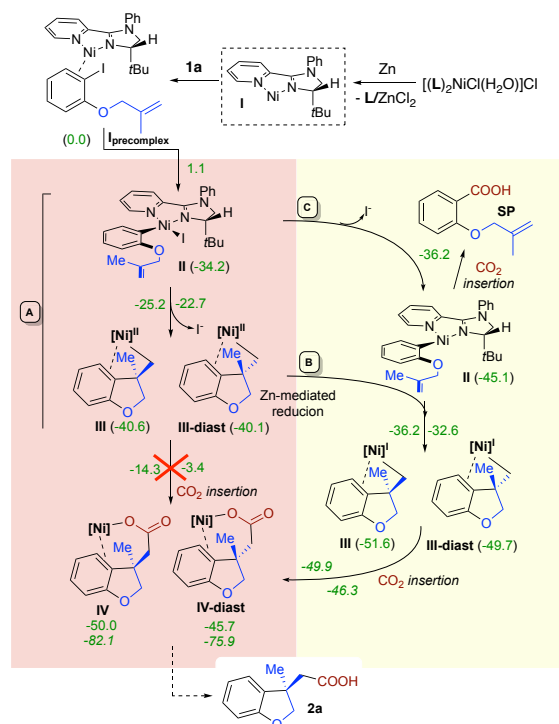
Scheme 3. Reaction mechanism explored via density functional theory. A relative-free-energies computed at the PCM(DMF)-M06/Def2SVPP level of theory at 1 atm and 298 K. See the Supporting Information for simulation details

This finding led us to conclude that indeed the isolated [(**L11**)$_2$Ni(H$_2$O)Cl]Cl species should be considered a pre-catalytic unit, capable of delivering the active 1:1 active organometallic species through an *in situ* ligand dissociation event.

Non-covalent interactions (NCI) analysis performed onto transition states **TS$_{II-III}$** and **TS$_{II-IIIdiast}$** provides an interesting picture of the stereodiscriminating mechanism where the *t*Bu group location is pivotal to differentiate between the two available trajectories for the cyclization (Figure 3). In both cases there is steric contact with this group, however, it is considerably stronger in the Ω trajectory than in the U alternative. In the former the *t*Bu group is pushed back by the incoming alkene which also translates into stronger steric contacts with the heterocyclic fragment of the chiral ligand in the back.
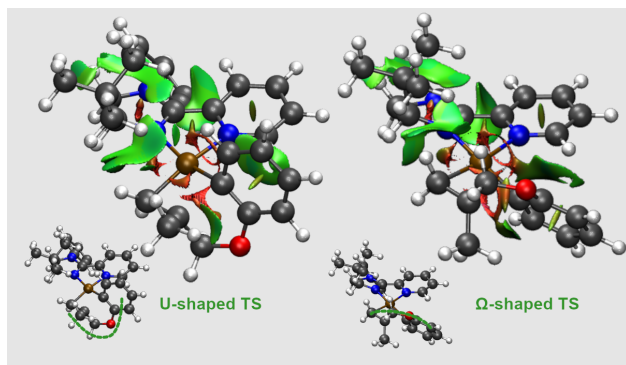
Figure 3. Non-covalent interactions for the favoured (U-shaped, left) and disfavoured (Ω-shaped, right) approaching trajectories of the C-Ni insertion to the double bond.

The strong impact of a methyl group in **L5** (Table 1, entry 5) was also diagnosed via NCI analysis and the crucial role of the solvent (*i.e.* DMF) on CO$_2$ activation was explained through a DFT model as well. Detailed answers to these points are provided in the Supporting Information.

In conclusion, an enantioselective nickel catalyzed tandem Heck-coupling/CO$_2$-carboxylation reaction is documented and its scope was evaluated to be wide enough to provide an unprecedented and versatile protocol for the synthesis of stereodefined hetero-benzofused acetic acids. A fully elucidated mechanistic profile, comprising an unusual Ni(I)-mediated Heck-type elementary step, was also proposed based on a combined experimental/computational analysis. Attempts to extend the present organometallic enantioselective strategy to the construction of differently and densely functionalized carboxylic acid derivatives through CO$_2$ fixation are underway in our laboratory and the results will be documented in due course.

[1] For representative reviews and monographs see: a) M. Aresta, *Carbon Dioxide as Chemical Feedstock*, Wiley-VCH: Weinheim, **2010**; b) T. Sakakura, J.-C. Choi, H. Yasuda, *Chem. Rev.* **2007**, *107*, 2365-2387; c) Y. Tsuji, T. Fujihara *Chem. Commun.* **2012**, *48*, 9956-9964; d) M. Aresta, A. Dibenedetto, A. Angelini, *Chem. Rev.* **2014**, *114*, 1709-1742; d) B. Yu, L.-N. He, *ChemSusChem* **2015**, *8*, 52-62; e) J. R. Cabrero-Antonino, R. Adam, M. Beller, *Angew. Chem. Int. Ed.* **2019**, *58*, 12820-12838; *Angew. Chem.* **2019**, *131*, 13137-13177.

[2] a) Q. Liu, L. Wu, R. Jackstell, M. Beller, *Nat. Commun.* **2014**, 1-15; b) C. S. Yeung, V. M. Dong, *Top. Catal.* **2014**, *57*, 1342-1350; c) C. Maeda, Y. Miyazaki, T. Ema, *Catal. Sci- Technol.* **2014**, *4*, 1482-1497; d) A. Tortajada, F. Julia-Hernandéz, M. Borjesson, T. Moragas, R. Martin, *Angew. Chem. Int. Ed.* **2018**, *57*, 15948-15982; *Angew. Chem.* **2018**, *130*, 16178-16214.

[3] For general reviews see: a) D. Yu, S.P. Teong, Y. Zhang, *Coord. Chem. Rev.* **2015**, *293*, 279-291; b) M. Borjesson, T. Moragas, D. Gallego, R. Martin, *ACS Catal.* **2016**, *6*, 6739-6749; c) S. Wang, G. Du, C. Xi, *Org. Biomol. Chem.* **2016**, *14*, 3666-3676; d) J. Luo, I. Larrosa, *ChemSusChem* **2017**, *10*, 3317-3332; e) I. Tommasi, *Catalysts*, **2017**, *7*, 380; f) J. Song, Q. Liu, H. Liu, X. Jiang, *Eur. J .Org. Chem.* **2018**, 696-713.

[4] a) L. Wang, W. Sun, C. Liu, *Chin. J. Chem.* **2018**, *38*, 353-362; b) L. Song, Y.-X. Jiang, Z. Zhang, Y.-Y. Gui, X.-Y. Zhou, D.-G. Yu, *Chem. Commun.* **2020**, *56*, 8355-8367.

[5] a) N. Kielland, C. J. Whiteoak, A. W. Kleij, *Adv. Synth. Catal.* **2013**, *355*, 2115-2138; b) X.-B. Lu, *Top. Organomet. Chem.* **2016**, *53*, 171-198; c) J. Vaitla, Y. Guttormsen, J. K. Mannisto, A. Nova, T. Repo, A. Bayer, K. H. Hopmann, *ACS Catal.* **2017**, *7*, 7231-7244.

[6] a) N. Negoro, S. Sasaki, S. Mikami, M. Ito, M. Suzuki, Y. Tsujihata, R. Ito, A. Farada, K. Takeuchi, N. Suzuki, J. Miyazeki, T. Santou, T. Odani, N. Kanzaki, M. Funami, T. Tanaka, A. Kogame, S. Matsunaga, T. Yasuma, Y. Momose, *ACS Med. Chem. Lett.* **2010**, *1*, 290-294; b) M.B. Vekariya, H.S. Joshi, N.C. Desai, K.A. Jadeja, *ChemistrySelect* **2019**, *4*, 10381-10384.

[7] For racemic syntheses see: a) S. Olivero, E. Dunach, *Eur. J. Org. Chem.* **1999**, 1885-1891; b) H. Senboku, J. Michinishi, S. Hara, *Synlett*, **2011**, *11*, 1567-1572.

[8] a) A. Cerveri, S. Pace, M. Monari, M. Lombardo, M. Bandini, *Chem. Eur. J.* **2019**, *25*, 15272-15276; b) Y. Liu, A. De Nisi, A. Cerveri, M. Bandini, *Org. Lett.* **2017**, *19*, 5034-5037; c) Y. Liu, A. Cerveri, A. De Nisi, M. Monari, O. Nieto Faza, C. Silva Lopez, M. Bandini, *Org. Chem. Front.* **2018**, *5*, 3231-3239; e) Y. Liu, M. Daka, M. Bandini, *Synthesis*, **2018**, *50*, 3187-3196.

[9] For a collection of seminal Ni-catalyzed fixations of CO$_2$ see: a) C. Amatore, A. Jutand, *J. Am. Chem. Soc.* **1991**, *113*, 2819-2825; b) M. Takimoto, K. Shimizu, M. Mori, *Org. Lett.* **2001**, *3*, 3345-3347; c) M. Takimoto, Y. Nakamura, K. Kimura, M. Mori, *J. Am. Chem. Soc.* **2004**, *126*, 5956-5957; d) T. Fujihara, K. Nogi, T. Xu, J. Terao, Y. Tsuji, *J. Am. Chem. Soc.* **2012**, *134*, 9106-9109; e) Y. Liu, J. Cornella, R. Martin, *J. Am. Chem. Soc.* **2014**, *136*, 11212-11215; f) F. Juliá-Hernández, T. Moragas, J. Cornella, R. Martin, *Nature*, **2017**, *545*, 84-89.

[10] For a general review see: S. Bhakta, T. Ghosh, *Adv. Synth. Catal.* **2020**, *362*, 5257-5274.

5

[11]   a) D. Olivero, *Eur. J. Org. Chem.* **1999**, 1885-1891; b) F. A. Siqueira, J. C. Taylor, C. R. D. Correia, *Tetrahedron Lett.* **2010**, *51*, 2101-2102; c) H. Senboku, J. Michinishi, S. Hara, *Synlett*, **2011**, 1567-1572.

[12]   a) W. You, M. K. Brown, *J. Am. Chem. Soc.* **2015**, *137*, 14578-14581; b) K. Wang, Z. Ding, Z. Zhou, W. Kong, *J. Am. Chem. Soc.* **2018**, *140*, 12364-12368; c) B. Ju, S. Chen, W. Kong, *Chem. Commun.* **2019**, *55*, 14311-14314; d) Y. Jin, C. Wang, *Angew. Chem. Int. Ed.* **2019**, *58*, 6794-6799; *Angew. Chem.* **2019**, *131*, 6342-6345; e) Z.-X. Tian, J.-B. Qiao, G.-L. Xu, X. Pang, L. Qi, W.-Y. Ma, Z.-Z. Zhao, J. Duan, Y.-F. Du, P. Su, X.-Y. Liu, X.-Z. Shu, *J. Am. Chem. Soc.* **2019**, *141*, 7637-7643; f) Z.-M. Zhang, B. Xu, L. Wu, Y. Wu, Y. Qian, L. Zhou, Y. Liu, J. Zhang, *Angew. Chem. Int. Ed.* **2019**, *58*, 14653-14659; *Angew. Chem.* **2019**, *131*, 13261-13266; g) Yang, F.; Jin, Y.; Wang, C. *Org. Lett.* **2019***, 21,* 6989-6994; h) Y. Jin, H. Yang, C. Wang, *Org. Lett.* **2020**, *22*, 2724-2729; i) J. He, Y. Xue, B. Han, C. Zhang, Y. Wang, S. Zhu, *Angew. Chem. Int. Ed.* **2020**, *59*, 2328-2332; *Angew. Chem.* **2020**, *132*, 2348-2352.

[13]   a) C. Karmel, C. Z. Rubel, E.V. Kharitonova, J. F. Hartwig, *Angew. Chem. Int. Ed.* **2020**, *59*, 6074-6081; *Angew. Chem.* **2020**, *132*, 6130-6137; b) Y. He, C. Liu, L. Yu, S. Zhu, *Angew. Chem. Int. Ed.* **2020**, *59*, 21530-21534; *Angew. Chem.* **2020**, *132*, 9271-9276.

[14]   For some representative examples see: a) T. Fujihara, K. Nogi, T. Xu, J. Terao, Y. Tsuji, *J. Am. Chem. Soc.* **2012**, *134*, 9106-9109; b) F. Rebih, M. Adreini, A. Moncomble, A. Harrison-Marchand, J. Maddaluno, M. Durandetti, *Chem.-Eur. J.* **2016**, *22*, 3758-3760; c) A. Correa, T. León, R. Martin, *J. Am. Chem. Soc.* **2014**, *136*, 1062-1069; c) C. Ma, C.-Q. Zhao, X.-T. Xu, Z.-M. Li, X.-Y. Wang, K. Zhang, T.S. Mei, *Org. Lett.* **2019**, *21*, 2464-2467; d) T. Yanagi, R. J. Somerville, K. Nogi, R. Martin, H. Yorimutsu, *ACS Catal.* **2020**, *10*, 2117-2123.

[15]   For general reviews on the topic see: a) T. Fan, X. Chen, Z. Lin, *Chem. Commun.* **2012**, *48*, 10808-10828; b) M. Obst, L. Pavlovic, K. H. Hopmann, *J. Organomet. Chem.* **2018**, *864*, 115-127

[16]   Among all the solvents tested, DMF was the only one effective in the carboxylation reaction.

[17]   a) C. Girard, H. B. Kagan, *Angew. Chem., Int. Ed.* **1998**, *37*, 4000-4037; *Angew. Chem.* **1998**, *110*, 3088-3127; b) H.B. Kagan, *Adv. Synth. Catal.* **2001**, *343*, 227-233.

[18]   J. B. Diccianni, T. Diao, *Trends in Chem.* **2019**, *1*, 830-844.

[19]   a) R. J. Somerville, R. Martin, *in* Nickel catalysis in organic synthesis: methods and reactions, chap. 12, pp. 285-330, Wiley-VCH, **2019**; b) F. B. Sayyed, Y. Tsuji, S. Sakaki, *Chem. Commun.* **2013**, *49*, 10715-10717.

[20]   M. Börjesson, T. Moragas, D. Gallego, R. Martin, *ACS Catal.* **2016**, *6*, 6739-6749.